AUTOMATIC CONTROL OF A SUPERSONIC AIR INLET WITH VARIABLE INNER CROSS-SECTION

Alexandru-Nicolae TUDOSIE[*], Elena - Elisa DRAGOMIR[**], Daniel - Cristian DRAGOMIR[*]

[*]University of Craiova, Romania (atudosie@elth.ucv.ro, dragomir.daniel.g6u@student.ucv.ro),
[**]In Flight Test Research and Innovation Center, Craiova, Romania (dragomir_elisa@yahoo.com)

DOI: 10.19062/2247-3173.2025.26.16

Abstract: *The paper deals with a planar supersonic air inlet with variable inner cross-section, equipped with a fixed geometry centerbody. Its optimal architecture is determined and possible control laws are studied. A control system was presented and modeled, based on the inlet's inner minimum cross-section opening control with respect to the flight regime. System's quality was estimated by some Matlab-Simulink simulations; control system's step response(s) for different flight regime's step input(s) were evaluated, which has permitted important conclusions, discussions and comments to be presented, concerning embedded system's properties an quality.*

Keywords: *inlet, Laval-nozzle, shock-wave, pressure ratio, control, step input.*

1. INTRODUCTION

Supersonic aircraft, because of their need of high-thrust, are equipped with air-breathing engines with afterburning (turbojet- or turbofan-type). Such propulsion systems require large mass airflows, air pressures, velocities and temperatures in front of the compressor as uniform as possible. This desire may be realized by using suitable air inlets; an air inlet, as the first organ of interaction between the engine and the atmosphere, has both connection and correlation important roles: it must transform the air free-stream parameters into suitable air parameters for engine's use, to keep it in a stable operation mode ([1], [2] and [3]).

The higher the flight speed of the supersonic aircraft, the more complex, better designed and manufactured its air inlet must be. In order to assure the necessary air flow for the engine, the supersonic inlet must tune itself to any flight regime (flight speed and altitude, expressed by the aircraft's flight Mach number) and to any engine operating regime (given by engine's rotational speed) ([2], [4] and [5]).

Aircraft designers and manufacturers must choose the inlet's architecture considering the aircraft role (civilian or military purpose), its flight regime (the flight Mach number, speed and altitude), as well as the inlet positioning on the aircraft's frame. According to these requests, different architectures might be chosen: frontal inlets with conical mobile centerbodies, rectangular inlets with/without mobile ramp(s), diverterless inlets or Pitot intakes ([2], [3] and [4]). The option for a certain inlet type and for its control necessity and possibilities is based on the exact knowledge of the aircraft role, the estimated lifespan and the desired level of safety.

Supersonic air inlets have inner and outer complex flows, where shock waves, interfered waves and/or expansion waves might occur.

Likewise, interactions between the shock waves and the boundary layer, early flow separation, as well as buzz/stall instability etc may appear, which may affect the overall operation of the entire propulsion system.

Consequently, inlets' design is an important issue, because it involves not only theoretical studies, but also both deep experimental analysis, meant to better highlight and understand their flow-field, in order to better predict their behavior during a large range of flight regimes (from low subsonic to high supersonic velocity) and to establish their operational characteristics.

The air inlet calculation and design approach has two directions: the 2D approach ([6] and [7]) - suitable for rectangular inlets, provided with fixed or mobile flat panels, or for axisymmetric inlets, and the 3D approach ([8] and [9]) - suitable for a large class of asymmetrical inlets. However, phenomena specific to the 3D approach can also be encountered in some stages of operation of 2D (planar or axisymmetric) inlets, for example due to some particular flows (cross flows and sidewall), flow separation and/or shock wave-boundary layer interaction, which sometimes might be considerable, and induce supplementary loses and drag forces (as stated in [6], [7], [8] and [9]).

The control laws of these inlets must take into account all these observations; therefore, the shape, dimensions and control method must be chosen carefully. For planar inlets, provided with mobile panels or with sliding spikes, control (adjusting) laws and control methods were determined, as described in [4], [10], and [11] and [12]. Similarly, for axisymmetric inlets, control laws and methods were determined and studied in [4] and [13]. A different type of inlet is the one with inner compression, of Laval-nozzle shape, described and studied in [14], but difficult to use because of its lack of adaptability. However, its particular shape is often used in other types of inlets.

2. PROBLEM FORMULATION

Supersonic air inlets with mixed compression (both external and internal) are built with two different zones: a) the outerl zone, where the centerbody (wedge or spike) triggers a system of shock-waves (oblique- or conic-type); b) the internal (inner) zone, also known as the flow channel, which is often built and profiled similarly to a Laval-nozzle. Both supersonic inlets (with mixed compression and with inner supersonic buffer zone) have an inner normal shock wave (developed at the throat- the minimum section area zone, or slightly behind it, in the divergent zone of the inlet's channel), which position is determined by the flight regime (through the amount of the total pressure after the outer shock waves) and by the engine's operating regime (through the amount of the static pressure in front of the engine's compressor). Behind this normal shock-wave the air flow becomes subsonic and continue decelerates (because of channel's divergent shape) until it reaches the compressor.

An important issue of this kind of supersonic inlets is their activation, or their "starting", which means the generation of the inner normal shock-wave and then maintaining it in the desired area throughout the operation of the inlet-engine tandem, at any flight regime and at any engine speed.

This paper intends to study a supersonic air inlet with external fixed geometry and variable inner cross-section (as Fig. 1.a shows), in order to determine its control law and to evaluate the behavior of its automatic control system's performance.

A similar study was performed earlier, for an inlet presented in [14], but using a control law for an inner sliding diaphragm, useful for axisymmetric inlets. However, it is quite difficult (virtually impossible) to design an adjustable throat for an axisymmetric air inlet, in order to adapt it to various flight altitudes/speeds, so the solution developed in [14] is the only one to be applied.

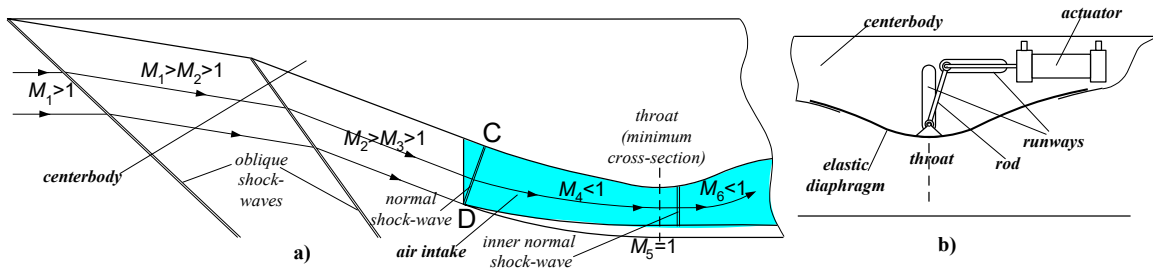

FIG. 1. Supersonic air inlet with fixed geometry centerbody and variable geometry throat

And yet, it is possible to build such a variable throat for a planar parallel inlet; it can be manufactured based on a much simpler geometry, since the cross-section of a rectangular shape with constant depth may be scaled by scaling only the other dimension of the rectangle (the height), as shown in Fig.1.b.

3. SUPERSONIC INLET GEOMETRY

As Fig. 1 shows, the studied inlet has a wedge-shape centerbody, which triggers the outer oblique shock-waves' system, while the intake's lip triggers a normal shock-wave, behind which the flow becomes subsonic; inside the rectangular flow channel the elastic diaphragm assures channel's Laval-shape by forming its throat of variable opening. Thus, the flow initially accelerates, becomes sonic at the throat and then jumps into subsonic through the normal shock-wave near the throat.

In fact, the most important phenomenon is the "starting" of the Laval-shape zone. The process with its challenges and its limits was presented in [14] and partly in [15]. Its initial conditions depends on the flow velocity and pressure behind the outer shock-waves system, as determined in [4], in [10] or in [13].

3.1. Inlet's outer configuration. As presented in [10], the optimal inlet configuration (as in Fig. 2) must define the geometry of the centerbody, which is obtained using an algorithm based on the Oswatitch condition, consisting of the total pressure recovery maximization. The total pressure recovery coefficient of the inlet is the product of the pressure recovery coefficients of the shock-waves:

$$\sigma_i^* = \sigma_{osw1}^* \sigma_{osw2}^* \sigma_{nsw}^* \sigma_d^*, \tag{1}$$

where σ_{osw1}^*, σ_{osw2}^* are oblique shock-waves' total pressure recovery ratios, σ_{nsw}^* – normal shock-wave's total pressure recovery ratio and σ_d^* – total pressure recovery ratio inside the channel (which can be considered constant, independent of flight and engine operation modes).

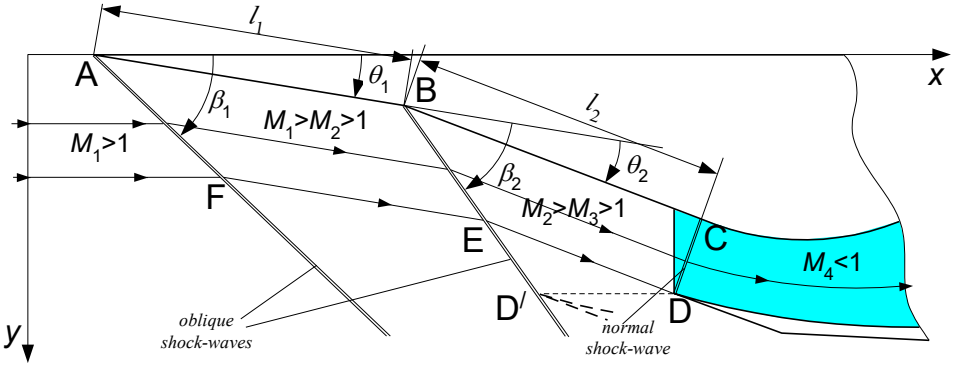

FIG. 2 Supersonic inlet outer configuration

These values must be calculated together with the other shock-waves parameters, using specific formulas:

- for the oblique shock waves

$$\sin^2\beta_k = \frac{1}{M_k^2} + \frac{\chi+1}{2}\frac{\sin\beta_k \cdot \sin\theta_k}{\cos(\beta_k\text{-}\theta_k)}, \tag{2}$$

$$M_{k_{av}}^2 = \frac{1}{\sin^2(\beta_k-\theta_k)}\frac{(\chi-1)M_k^2\sin^2\beta_k+2}{2\chi M_k^2\sin^2\beta_k-(\chi-1)}, \tag{3}$$

$$\sigma_{oswk}^* = \left[\frac{(\chi+1)M_k^2\sin^2\theta_k}{2+(\chi-1)M_k^2\sin^2\theta_k}\right]^{\frac{\chi}{\chi-1}}\left[\frac{\chi+1}{2\chi M_k^2\sin^2\theta_k-(\chi-1)}\right]^{\frac{1}{\chi-1}}, \tag{4}$$

where $k=\overline{1,2}$, M_k – Mach number in front of the shock-wave, $M_{k_{av}}$ – Mach number behind the shock-wave; θ_k – centerbody's flare angles, β_k – shock-waves' angles, χ – air's adiabatic exponent.

- for the normal shock-wave

$$M_{av}^2 = \frac{(\chi-1)M_k^2+2}{2\chi M_k^2-(\chi-1)}, \tag{5}$$

$$\sigma_{nsw}^* = \left[\frac{(\chi+1)M_k^2}{2+(\chi-1)M_k^2}\right]^{\frac{\chi}{\chi-1}}\left[\frac{\chi+1}{2\chi M_k^2-(\chi-1)}\right]^{\frac{1}{\chi-1}}, \tag{6}$$

where M_k – Mach number in front of the normal shock-wave, M_{av} – Mach number measured after the normal shock-wave.

For a flight Mach number $M_1=2.1$ considered as Mach in front of the inlet, applying the above described algorithm in order to maximize the total pressure recovery σ_i^*, one has obtained the optimal flare angles: $\theta_{1_{opt}}=11.14^\circ$, $\theta_{2_{opt}}=12.22^\circ$. The other geometrical elements are calculated as $l_1=0.8849$, $l_2=0.7624$, while characteristic points in Fig. 2 have the coordinates:
$A(0;0); B(0.874;0.142); C(1.569;0.454); D(1.324;1)$.

For lower upstream Mach numbers, $M_1^{/}<M_{1_{nom}}$, the intensity of both external oblique shock-waves is decreasing, so they are depleting and their angles β_1 and β_2 are consequently growing, which also leads to the pressure recovery coefficient σ_i^* modifying.

3.2. Inlet's inner Laval-nozzle. As presented in [14], an intake with inner compression of Laval-nozzle shape must be activated by a favorable sequence of closing/openings of the minimum section (throat).

One assume that the nozzle geometry (A_{cr} - the throat area and A_e - the exit area, as well as the variation of nozzle's cross section area versus its length $A=A(x)$) is known, then the air flow rate $\dot{m}_a$ passing through the nozzle is also known as supplied by the outer part of the inlet, as well as the upstream air's parameters (pressure p^* and temperature T^* or enthalpy i^*).

Applying the Saint-Venant equation (as presented in [2]), considered for the important sections (throat and exit section), one may obtain

$$\beta_e^{\frac{2}{\chi}}\left(1-\beta_e^{\frac{\chi-1}{\chi}}\right)=\frac{\chi-1}{2}\left(\frac{2}{\chi+1}\right)^{\frac{\chi+1}{\chi-1}}\left(\frac{A_{cr}}{A_e}\right)^2, \tag{7}$$

where $\beta_e=\frac{p_e}{p^*}$ is the pressure ratio; it may be calculated if p_e (static pressure in front of the engine) and p^* (total pressure after the outer shock-wave system) are known. The two roots of the equation (7) are: the first for the subsonic mode $\beta_e^{/}>\beta_{cr}$, the second for the supersonic mode $\beta_e^{/}<\beta_{cr}$, where $\beta_{cr}=\left(\frac{2}{\chi+1}\right)^{\frac{\chi}{\chi-1}}$; each one corresponds to a pressure value in the exit section $p_e^{/}$, respectively $p_e^{//}$.

For a pressure in front of the engine $p_e \geq p_e^{/}$, the flow mode inside the nozzle is completely subsonic (see curves 1, 2, 3 in Fig. 3). The curve 3 is reached when the pressure value becomes equal to $p_e^{/}$ (it is the limit curve of the subsonic flow). If the pressure value is $p_e<p_e^{//}$, the flow mode in the divergent zone becomes supersonic (curve 4) and the Laval nozzle is considered completely started. When $p_e^{//}<p_e<p_e^{/}$ a mixed flow mode occurs in the nozzle's divergent zone, where a normal shock wave might appear.

One may restrain the pressure range even more, considering the nozzle's starting as complete if the above-mentioned normal shock-wave appears in nozzle's output section. Applying the flow rate equation where one has chosen the solution $\left(\lambda_e^{///}>1\right)$, the velocity coefficient before the shock-wave ($\lambda_e^{///}$) can be calculated as

$$q\left(\lambda_e^{///}\right)=\frac{\dot{m}\sqrt{T^*}}{KA_e p^*}, \tag{8}$$

while the velocity coefficient behind the shock-wave is $\frac{1}{\lambda_e^{///}}$ and the flow rate function is

$$q(\lambda)=\lambda\left[\frac{\chi+1}{2}\left(1-\frac{\chi-1}{\chi+1}\lambda^2\right)\right]^{\frac{1}{\chi-1}}. \tag{9}$$

Through the normal shock-wave the total pressure drops so, behind it, on may calculate the pressure using the flow conservation equation, as folows

$$p_{av}^*=\frac{\dot{m}\sqrt{T^*}}{KA_e q\left(\frac{1}{\lambda_e^{///}}\right)}, \tag{10}$$

The limit-value of the outer pressure $p_e^{///}$ (in front of engine's compressor), below which one may consider the de Laval nozzle as fully started, may be calculated from

$$p_e^{///} = p_{av}^* \Pi\left(\frac{1}{\lambda_e^{///}}\right) = \left[\dot{m}\sqrt{T^*}\,\Pi\left(\frac{1}{\lambda_e^{///}}\right)\right] / \left[KA_e q\left(\frac{1}{\lambda_e^{///}}\right)\right], \tag{11}$$

where $\Pi(\lambda) = 1 - \frac{\chi - 1}{\chi + 1}\lambda^2$ is the thermodynamic funcion of the pressure.

Thus, depending on the static pressure's value downstream of the divergent zone of the Laval nozzle, during its starting three different situations may occur:

a) if $p_e \geq p_e^{/}$ the nozzle is totally under subsonic flow;

b) if $p_e^{/} > p_e > p_e^{///}$ a mixed flow appears in its divergent zone, where a normal shock-wave is triggered; its upstream flow is supersonic, then subsonic downstream (see Fig. 3, curve 5);

c) if $p_e < p_e^{///}$, the normal shock-wave is completely evacuated from the divergent zone of the nozzle, and, consequently, the nozzle is fully started.

The emergence of a normal shock-wave in Laval nozzle's divergent zone (case b) - corresponding to curve 5 in Fig. 3) raises an important issue to be studied: the determination of its position. As far as the upstream (p^*, T^*) and downstream (p_e)parameters are dtermined by the operational regimes and the variation of nozzle section its longitudinal coordinate $A = A(x)$ is also known, one has to determine the shock-wave position measured from the throat (or from the nozzle's entry). Firstly, the pressure will drop, following the curve 4, in the initial part of the nozzle, being supersonic up to the shock-wave. The pressure undergoes a jump through the normal shock-wave, then it follows the curve 5 in Fig. 3 untill the exit section, where it reaches the value p_e.

3.3. Inlet's control law. The work line of the inlet has precise positioning, as Fig. 4 shows. Possible control laws of the inlet were determined in [14] and [4]. The limits of the working lines are the curves I and II; between them all control laws should be developed. However, not all of these laws are suitable for this type of inlet, since the upstream flow velocity varies differently due to the presence of the oblique shock-waves.

The control law must consider some important situations, as follows:

a) the start of the engine, which corresponds to point A. The whole inlet must be completely open, so its throat (the critical area) should have the maximum area;

b) the acceleration, until the upstream reaches the sound speed (the slice A-B in Fig. 4). The inlet's throat must keep the same maximum opening. When the sound speed was reached, a normal shock wave is triggered in front of the air inlet; however, the air intake meets a subsonic flow and the inlet is still working in subsonic mode;

c) acceleration in the supersonic mode, section B-C, until the shock wave is triggered in the throat zone. Continuing the acceleration, one must gradually reduce the throat (see curve I), with respect to the air speed increasing. Shock-wave's position must be stabilized once reaching the Mach number limit, so the minimum section (the throat) must close, until the point D, close to the second limit curve (II); a certain reserve must be kept from curve II, in order not to disable (to „deactivate") the intake. However, the position of points C and D are determined knowing the flight Mach number value. Further acceleration must be done following the curve EF, near the first border curve I, or to maintain the opening of the point E;

d) when the oblique shock-waves of the outer inlet's configuration are detaching, the conditions of the upstream flow are changing and the "reopening" of the throat is necessary, so the control law must follow the path DC or a new path from E to C on the first border curve.

Considering these observations, one must choose the control law so that the shock wave inside the channel is maintained in the throat area, behind it. Consequently, the control parameter of the inlet must be connected to this shock-wave; the most important parameter is the total pressure recovery, but it might be replaced with the pressure ratio φ_m between the total and the static pressure, which indirectly gives information about the Mach number in the throat zone M_5:

$$\varphi_m = \frac{p_m^*}{p_m} = \left(1 + \frac{\chi - 1}{2} M_5^2\right)^{\frac{\chi}{\chi - 1}}. \tag{12}$$

So, this parameter must be measured and a control system based on it may be imagined, which must open/close the throat with respect to the flow conditions in the throat zone.

4. INLET'S CONTROL SYSTEM'S ARCHITECTURE

The operational block diagram is depicted in Fig. 5, which explains the way of action of the control system, while the architecture of inlet's automatic control system is depicted in Fig. 6. The control system is equipped with an elastic diaphragm with pressure intakes; this diaphragm assures the variation of throat's cross-section, being moved by the hydraulic actuator.

The position of both pressure intakes was chosen to facilitate the measuring of both mean total pressure p_m^* and mean static pressure p_m at throat's level. From aerodynamic and thermodynamic points of view, the pressures' ratio φ_m is a function of M_5 - the upstream Mach number, as Eq. (12) shows. Inlet's control law is non-linear-type; however, it could be linearized, but only accepting positioning errors, which leads to higher total pressure losses and, possibly, inlet's operational errors.

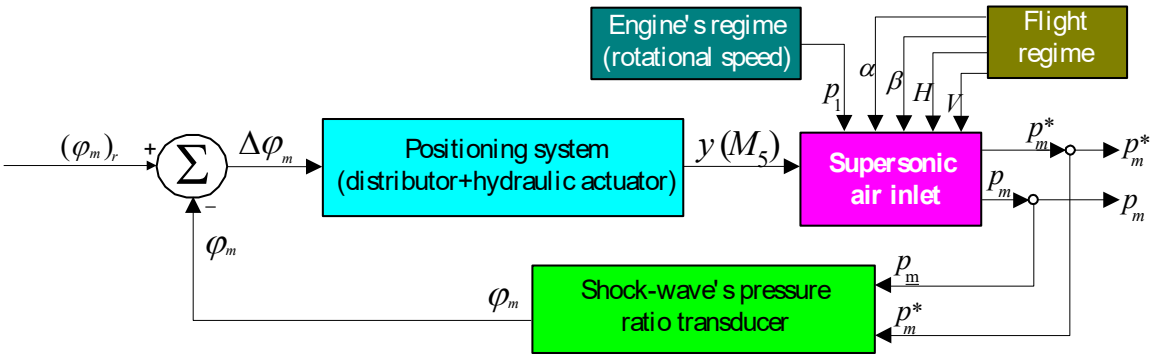

FIG. 5. Automatic control system's operational block diagram

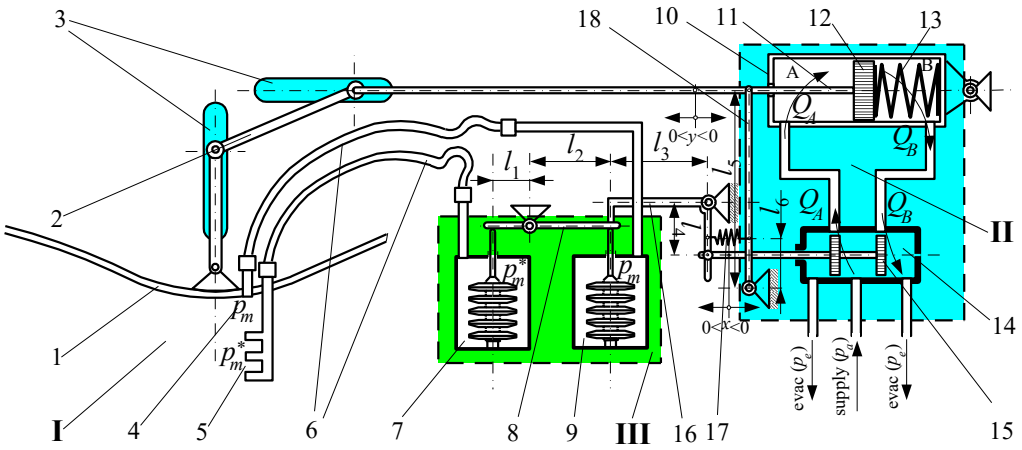

System's main parts:
I-supersonic inlet's throat area; **II**-actuator; **III**-pressure sensor;

1-elastic diaphragm; 2-rod; 3-runways; 4-static pressure intake; 5-total pressure intakes ramp; 6-flexible pipes; 7-total pressure sensor (capsules); 8-pressure sensor's lever; 9-static pressure sensor (with capsules); 10-hydraulic actuator (cylinder); 11-actuator's main rod; 12-actuator's piston; 13-actuator's spring; 14-distributor; 15-distributor's slide-valve; 16-rocking lever; 17-main feedback's spring; 18-main feedback's lever.

FIG. 6 Automatic control system's architecture

5. CONTROL SYSTEM'S MATHEMATICAL MODEL

The mathematical model of the control system consists of its main parts non-linear equations, as follows:

a) The equation of the pressure ratio's transducer:

$$S_{a1}l_1p_m^* - S_{a2}l_2p_m - \frac{l_2l_4}{l_3}\left(m\frac{\mathrm{d}^2x}{\mathrm{d}t^2} + \xi\frac{\mathrm{d}x}{\mathrm{d}t}\right) - (k_{r1}l_1 + k_{r2}l_2)x = 0, \tag{13}$$

where k_{r1}, k_{r2} – transducer's capsule's elastic constants; m – mobile rod and accessories mass; ξ – viscous friction co-efficient; l_1, l_2 – transducer's lever arms' length; l_3, l_4 – transducer's rocking lever arms' length; S_{a1}, S_{a2} – aneroid capsules surface areas (usually considered as equal $S_{a1} = S_{a2} = S_a$); x – distributor's slide-valve's displacement;

b) The equations of the actuator and of the distributor:

$$Q_A = \mu_a L_d x\sqrt{\frac{2}{\rho_{hf}}}\sqrt{p_a - p_A}\,, \tag{14}$$

$$Q_B = \mu_a L_d x\sqrt{\frac{2}{\rho_{hf}}}\sqrt{p_B - p_e}\,, \tag{15}$$

$$Q_A = S_p\frac{\mathrm{d}(y_r - y)}{\mathrm{d}t} + \beta_{hf}V_{A0}\frac{\mathrm{d}p_A}{\mathrm{d}t} \tag{16}$$

$$Q_B = S_p \frac{\mathrm{d}(y_r + y)}{\mathrm{d}t} - \beta_{hf} V_{B0} \frac{\mathrm{d}p_B}{\mathrm{d}t}, \tag{17}$$

$$S_p (p_A - p_B) = m_p \frac{\mathrm{d}^2(y + y_r)}{\mathrm{d}t^2} + \xi_f \frac{\mathrm{d}(y + y_r)}{\mathrm{d}t} + k_{ea}(y_r + y + y_0), \tag{18}$$

where Q_A, Q_B – hydraulic fluid's flow rates; μ_a – flow rate co-efficient; L_d – distributor's orifice's width; p_A, p_B – actuator's chambers' pressures; y – actuator's rod's displacement; V_A, V_B – transducer's chambers volume; β_{hf} – hydraulic fluid's compressibility co-efficient; k_{ea} – actuator's spring's elastic constant; m_p – actuator's mobile rod and accessories mass; ξ_f – viscous friction co-efficient; p_a – hydraulic fluid supplying pressure; p_e – fluid's pressure in the low pressure circuit (which may be neglected, because of its small value compared to p_A and p_B).

Obviously, this mathematical model (Eqs. (13) to (18)) is a non-linear one, not suitable for further studies. It must be brought to a linear form, then adimensionalized and, finally, submitted to the Laplace transformation. This algorithm was described in [4] and [16], and applied for studies in [10], [13], [14] and [15]. It uses the small perturbation hypothesis and the finite differences method, which considers any variable X as $X = X_0 + \Delta X$ and $\overline{X} = \frac{\Delta X}{X_0}$, where ΔX – deviation, X_0 – steady state regime's value and $\overline{X}$ – non-dimensional deviation.

Mathematical model's linearized dimensionless form has resulted as:

$$k_{mt} \overline{p}_m^* - k_m \overline{p}_m = \overline{x} \tag{19}$$

$$k_x \overline{x} - \tau_y \mathrm{s} \overline{y} = (\tau_{Ap} \mathrm{s} + 1)(\overline{p}_A - \overline{p}_B), \tag{20}$$

$$\overline{y} = k_y (\overline{p}_A - \overline{p}_B), \tag{21}$$

with the used notations

$$k_{Ax} = \mu_a L_d \sqrt{\frac{p_a - p_e}{\rho_{hf}}}, T_x = \sqrt{\frac{m l_2 l_4}{(k_{r1} l_1 + k_{r2} l_2) l_3}}, 2T_x \omega_0 = \frac{\xi\, l_2 l_4}{(k_{r1} l_1 + k_{r2} l_2) l_3}, T_y = \sqrt{\frac{m_p}{k_{ea}}},$$

$$2T_y \omega_0 = \frac{\xi_f}{k_{ea}}, k_{Ap} = \mu_a L_d x_0 \sqrt{\frac{1}{\rho_{hf}(p_a - p_e)}},$$

$$k_{xS} = \frac{S_a}{k_{r1} l_1 + k_{r2} l_2}, k_{px} = \frac{2k_{Ax}}{k_{Ap}}, \tau_{py} = \frac{2S_p}{k_{Ap}}, \tau_{Ap} = \frac{\beta_{hf} V_0}{k_{Ap}}, k_{py} = \frac{S_p}{k_{ea}}. \tag{22}$$

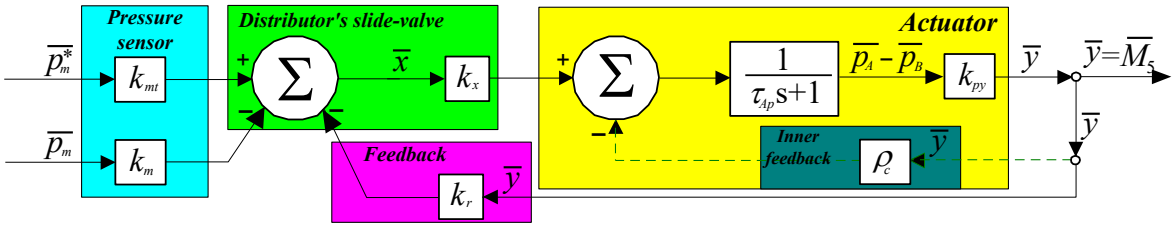

FIG. 7 Automatic control system's block diagram with transfer functions

$$k_{mt}=\frac{l_1 k_{xS} p^*_{m0}}{x_0},\ k_m=\frac{l_2 k_{xS} p_{m0}}{x_0}\approx k_{mt},\ k_x=\frac{k_{px}x_0}{p_{A0}},\ \tau_y=\frac{\tau_{py}y_0}{p_{A0}},\ k_y=\frac{k_{py}p_{A0}}{y_0}.$$

Assuming that the compressibility coefficients and the viscous friction coefficient may be neglected, the new (simplified) form of the mathematical model becomes:

$$k_x k_y\left(k_{mt}\bar{p}^*_m-k_m\bar{p}_m\right)=\left(k_y\tau_y\mathrm{s}+1\right)\bar{y}, \tag{23}$$

$$\bar{y}=\frac{k_x k_y}{\left(k_y\tau_y\mathrm{s}+1\right)}\left(k_{mt}\bar{p}^*_m-k_m\bar{p}_m\right)=\frac{k}{\left(\tau\mathrm{s}+1\right)}\left(k_{mt}\bar{p}^*_m-k_m\bar{p}_m\right). \tag{24}$$

that means that system's transfer function is a first order one, where the expressions of the time constant τ and of the gain co-efficient k are, as follows:

$$\tau=k_y\tau_y=\frac{2S_p^2\sqrt{\rho_{hf}\left(p_a-p_e\right)}}{k_{ea}\mu_a L_d x_0}, \tag{25}$$

$$k=k_x k_y=\frac{2S_p\left(p_a-p_e\right)}{k_{ea}y_0}. \tag{26}$$

Based on these equations, the block diagram with transfer functions was built, and is depicted in Fig. 7.

An important remark must be done, regarding the actuator's architecture. It might be used in its simple form, or it might contain an additional internal feedback for the purpose of improving performance, as studied in [10]; the inner feedback is highlighted in Fig. 7 inside the actuator with dashed line.

Consequently, the mathematical model changes, becoming:

$$\bar{y}=\frac{k_x k_y}{\left(k_y\tau_y\mathrm{s}+k_y\rho_s+1\right)}\left(k_{mt}\bar{p}^*_m-k_m\bar{p}_m\right)=\frac{k_1}{\left(\tau_1\mathrm{s}+1\right)}\left(k_{mt}\bar{p}^*_m-k_m\bar{p}_m\right), \tag{27}$$

with new forms of the time constant and of the gain:

$$\tau_1=\frac{k_y}{k_y\rho_s+1}\tau_y,\quad k_1=\frac{k_x k_y}{k_y\rho_s+1}. \tag{28}$$

Obviously, the system remains a first order – one, but its coefficients have received new forms and new values, both of them becoming smaller than for the basic system.

6. CONTROL SYSTEM'S STABILITY AND QUALITY EVALUATION

Both transfer functions of the studied system (with respect to each one of the input pressures), have, obviously, first order characteristic polynomials. Their expressions are:

$$H_{mt}(\mathrm{s}) = \frac{k_x k_y k_{mt}}{\left(k_y \tau_y \mathrm{s} + k_r\right)} \bar{p}_m^*,\ H_m(\mathrm{s}) = -\frac{k_x k_y k_m}{\left(k_y \tau_y \mathrm{s} + k_r\right)} \bar{p}_m . \tag{29}$$

Consequently, according to the Routh-Hurwitz criteria, in order to assure the stability of the control system, the polynomial coefficients must have the same sign, strictly positive in this particular case $\left(k_y \tau_y > 0 \text{ and } k_r > 0\right)$; these conditions lead to

$$l_1 > \frac{S_a p_{m0}^2 l_4}{p_{m0}^* \left(l_3 k_{r2} - l_3 k_{r1} + S_a p_{m0}\right)},\ l_2 > \frac{S_a p_{m0}^2 \left(S_a p_{m0} - l_3 k_{r1}\right)}{p_{m0}^* l_4 k_{r2} \left(l_3 k_{r2} - l_3 k_{r1} + S_a p_{m0}\right)} . \tag{30}$$

If it is chosen that the capsules have identical geometric parameters, one obtains for the minimum value of the lever arms:

$$l_1 = \frac{p_{m0}}{p_{m0}^*} l_3,\ l_2 = \frac{p_{m0}\left(S_a p_{m0} - l_3 k_r\right)}{p_{m0}^* k_r} \frac{l_4}{l_3} . \tag{31}$$

If the improved architecture of the actuator is chosen to be used, the stability conditions remain the same.

The quality of the automatic control system of the air inlet's internal cross-section is estimated, based on its transfer functions' form, by studying its response to the step input of the pressure parameters. The study was conducted for three values of the Mach number of flight in front of the inlet, namely for the maximum speed ($M_1 = 2.1$), for the situation of detachment of the second oblique shock wave ($M_1 = 1.7$), and for the situation of detachment of the first oblique shock wave ($M_1 = 1.438$).

System's step response is presented in Fig. 8. Both actuator configurations were used for the studies: the basic actuator (without internal feedback), but also the actuator with internal feedback. The system response was plotted with a solid line for the basic actuator, and with a dashed line for the improved actuator. Figures 8.a depict system's step response for $\bar{p}_m^*$ and constant $p_m\left(\bar{p}_m = 0\right)$ for different Mach numbers, while Fig.8.b depict system's step response for $\bar{p}_m$ and constant $p_m^*\left(\bar{p}_m^* = 0\right)$ for different Mach numbers.

As expected, all step response curves behave asymptotically, with static errors and various settling times values (as presented in Table 1).

Table 1. Static errors and settling times

	Step input parameter	$\bar{p}_m^*$ and constant $p_m\left(\bar{p}_m = 0\right)$		$\bar{p}_m$ and constant $p_m^*\left(\bar{p}_m^* = 0\right)$	
Flight Mach number	Actuator / Parameter	With feedback	Without feedback	With feedback	Without feedback
$M_1 = 2.1$	Static error	5.3%	4.7%	3.6 %	3 %
	Settling time	3.2 sec	2.6 sec	3.0 sec	2.0 sec
$M_1 = 1.7$	Static error	6.8%	5.6%	4.7%	3.8%
	Settling time	2.7 sec	2.3 sec	2.6 sec	1.6 sec
$M_1 = 1.438$	Static error	8.5%	7.2%	5.8%	4.8%
	Settling time	2.3 sec	1.9 sec	2.0 sec	1.4 sec

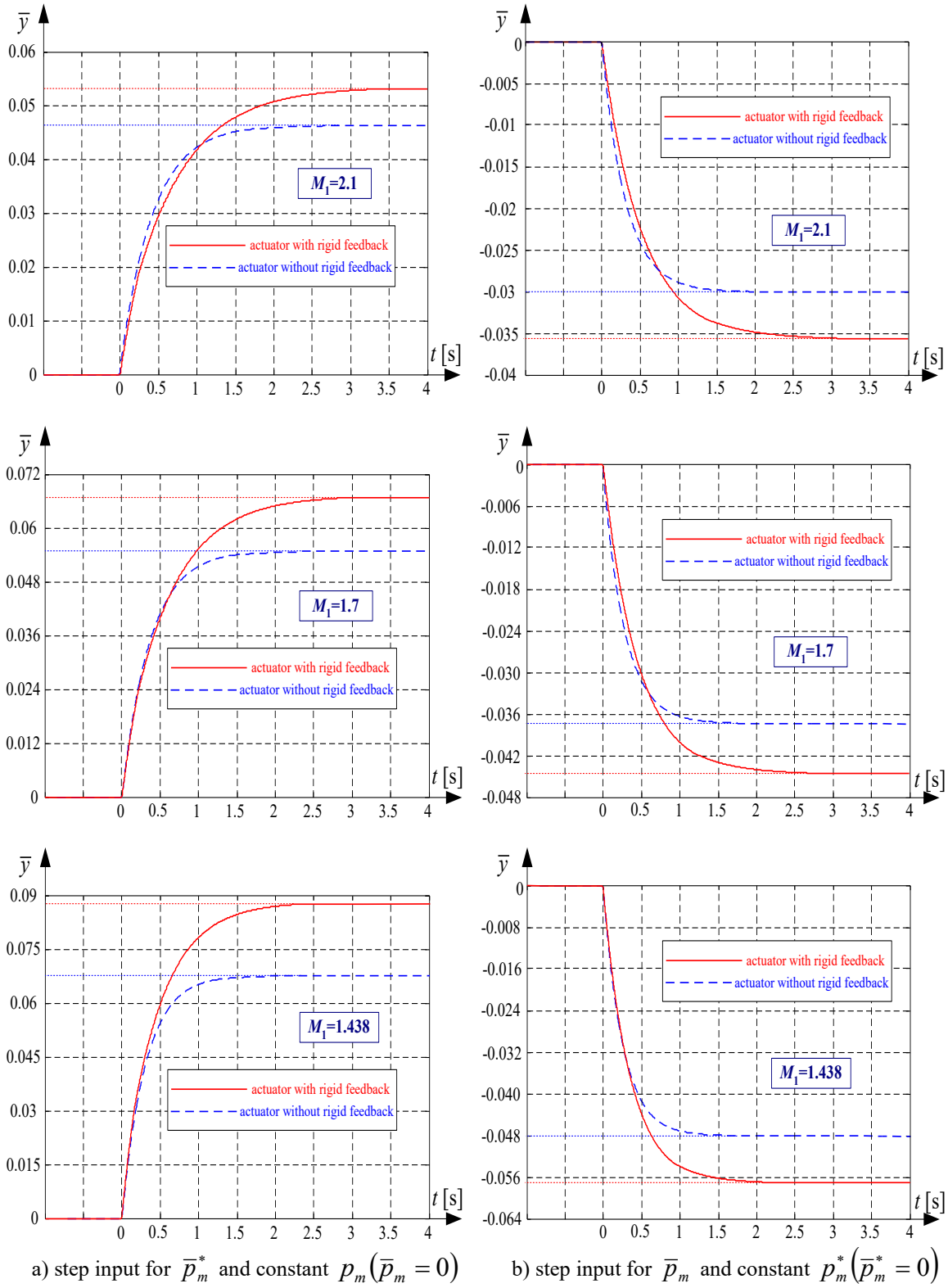

a) step input for $\overline{p}_m^*$ and constant $p_m\left(\overline{p}_m = 0\right)$ b) step input for $\overline{p}_m$ and constant $p_m^*\left(\overline{p}_m^* = 0\right)$

FIG. 8 System's step response for different Flight Mach numbers and different actuator's architecture

From studying the graphs in Fig. 8, the values of the static errors and settling times were determined; analyzing the results in Table 1, it can be stated that the flight regime has an important influence on the behavior of the automatic system. Thus, the more intense the flight regime (the higher the flight Mach number), the more the settling times

increase in value; however, automatic system's static errors have an opposite behavior, being smaller the more intense the flight regime. The static errors of the system in the case of step input of the static pressure parameter are negative, as expected from the transfer function form.

Both the settling times and the static errors are higher for the step input of the total pressure parameter than for the static pressure one; consequently, it can be stated that the flight mode influences more than the engine operating mode.

CONCLUSIONS

The paper studied a plan supersonic air inlet for aircraft use with variable inner cross-section and fix geometry centerbody as controlled object. Based on inlet's operation for different flight regimes, its optimal geometry for the centerbody was determined, as well as the conditions for inlet's activation (starting) using the inner flow channel's throat opening in order to preserve the normal shock-wave at the desired position and intensity.

Possible control laws for the inlet were discussed and the one that best suited the operating conditions of the inlet was chosen. In order to accomplish this task, an automatic control system for the throat's opening was issued, then described through its mathematical model. As controlled parameter of this system, the throat's opening (in fact the actuator's rod positioning) was obviously chosen; the control parameter was chosen between a lot of possibilities, but the pressure ratio through the inner shock-wave (proportional to the upstream flow's Mach number) was the first option.

The control system consists of a pressure ratio transducer and a hydraulic actuator; the pressure transducer is very important for the system's operation, because it should fulfill two main tasks: first of all - the sensing task (both pressures measuring), then the comparing task - to compare the measured pressure ratio to the preset pressure ratio value (which was determined from the construction along with the choice of the lengths of the lever arms). For the chosen system, the constructive values of the lever arms' length were determined from the condition of ensuring stability.

From studying the system's response to step input, it resulted that the system is always asymptotically stable, but with a static error, the value of which is all the greater the less intense the flight regime.

The system behavior was compared for the two possible actuator architectures (with or without internal rigid feedback); it resulted that the presence of an additional feedback, although it complicates the system architecture, has a beneficial influence on its operation, reducing both its settling times and its static errors.

The results may be used for inlet's control system pre-design, but for effective using of such a system, real-time experiments must be performed and corrections might be added.

REFERENCES

[1] J. D. Mattingly, *Elements Of Gas Turbine Propulsion*. McGraw-Hill, New York, 1996;
[2] V. Pimsner, *Air-breathing Jet Engines. Processes and Characteristics*, Bucharest, Didactic and Pedagogic Publishing, 1983;
[3] J. J. Seddon and E. L. Goldsmith, *Intake Aerodynamics*, 2nd edition, AIAA Education Series, 1999;
[4] A. N. Tudosie, *Aerospace Propulsion Systems Automation*. University of Craiova Inprint, 2005;
[5] L. C. Jaw and J. D. Mattingly, *Aircraft Engine Controls: Design, System Analysis, and Health Monitoring*, AIAA Education Series, 2009;
[6] C. Berbente and N. V. Constantinescu, *Gases Dynamics*, vol. I, II. Politehnica University in Bucharest Inprint, 1985;

[7] H. Ran and D. Mavris, Preliminary Design of a 2D Supersonic Inlet to Maximize Total Pressure Recovery, *in Proceedings of AIAA 5th Aviation, Technology, Integration and Operations Conference (ATIO)*, 26-28 Sept., Arlington, Virginia, 2005, pp. 1-11;

[8] Y. P. Goonko and E. Alexandrov, Aerodynamic Design Of A Supersonic Three-Dimensional Inlet, *in Thermophysics and Aeromechanics,* Vol. 1, Nr. 17, 2010, pp. 57-68;

[9] J. W. Slater, External-Compression Supersonic Inlet Design Code. *NASA 2011 Technical Conference*, Cleveland, Ohio, 2011;

[10] A. N. Tudosie and M. L. Paunescu. Automatic Control System for an Aircraft Plan Supersonic Inlet with Mobile Panel. *Proceedings of 19th International Conference of Scientific Paper "Scientific Research and Education in the Air Force",AFASES 2017*, Brasov, 25-27 May 2017, pp. 243-252; DOI: 10.19062/2247-3173.2017.19.1.27;

[11] A. N. Tudosie, Control Law for the Air Inlet of a High Supersonic Velocity Aerial Vehicle. *Proceedings of International Conference on Control, Artificial Intelligence, Robotics and Optimization*, DOI: 10.1109/ICCAIRO46080.2018, Prague, 19-21 May, 2018, pp. 6-13;

[12] Watanabe, Y. and Murakami, A. Control Of Supersonic Inlet With Variable Ramp, *Proceedings of 25th International Congress of The Aeronautical Sciences, ICAS 2006*, pp. 1-10, Hamburg, 3-8 Sept., 2006;

[13] I. Aron, and A. N. Tudosie, Hydromechanical system for the supersonic air inlet's channel's section control. *In Proceedings of International Conference on Applied and Theoretical Electricity*, Craiova, 2000, pp 266-269. ISBN-973-657-005-3;

[14] A. N. Tudosie, E. Dumitru and M. A. Aspra, Control Law For An Aircraft Supersonic Air Inlet With Internal Compression. *Proceedings of 21st International Conference of Scientific Paper "Scientific Research and Education in the Air Force",AFASES 2019*, Brasov, 28 May -2 June 2019, pp. 243-252; DOI:10.19062/2247-3173.2019.21.27;

[15] A. N. Tudosie, Supersonic Air Inlet's Control System Based On The Inner Normal Shock Wave's Position Stabilisation. *Proceedings of International Conference on Military Technologies ICMT 2007*, University of Defense, Brno, Czechia, May 3-5 2007, pp. 342-349;

[16] C. Rotaru, I. R. Edu, M. Andres-Mihaila and P. Matei, Applications of multivariable control techniques to aircraft gas turbine engines, in *Review of Air Force Academy*, no.2 (26), 2014, pp. 45-50.